Assessment of Breast Lesions With Diffusion-Weighted MRI: Comparing the Use of Different b Values

Fernanda Philadelpho Arantes Pereira[1,2,3]
Gabriela Martins[1,2]
Eduardo Figueiredo[4]
Marisa Nassar Aidar Domingues[1,2]
Romeu Cortes Domingues[1,2]
Lea Mirian Barbosa da Fonseca[1,3]
Emerson Leandro Gasparetto[1,2,3]

OBJECTIVE. Our purpose was to study the utility of diffusion-weighted MRI in differentiating benign from malignant breast lesions by assessing the best b values.

SUBJECTS AND METHODS. Forty-five women (mean age, 46.1 years) with 52 focal mass breast lesions underwent diffusion-weighted imaging with different b values. The apparent diffusion coefficient (ADC) value of each lesion was calculated from the ADC maps done using five b values (0, 250, 500, 750, and 1,000 s/mm^2) and using b values of 0 s/mm^2 with each other b value separately (0 and 250 s/mm^2, 0 and 500 s/mm^2, 0 and 750 s/mm^2, 0 and 1,000 s/mm^2). The mean ADC values were correlated with imaging findings and histopathologic diagnoses. The cutoff ADC value, sensitivity, and specificity of diffusion-weighted imaging to differentiate benign and malignant lesions were calculated in all b value combinations. A p value of < 0.05 was considered statistically significant.

RESULTS. The mean ADC value was significantly lower for malignant lesions compared to benign lesions ($p < 0.0001$) in all b value combinations. No statistical difference was seen between the ADC obtained from different b value combinations ($p = 0.2581$) in the differentiation between benign and malignant lesions. The ADC calculated from b 0 and 750 s/mm^2 was slightly better than the other b value combinations, showing a sensitivity of 92.3% and a specificity of 96.2%.

CONCLUSION. Diffusion-weighted imaging is a potential resource as a coadjutant of MRI in the differentiation between benign and malignant lesions. Such imaging can be performed without a significant increase in examination time, especially because it can be done with lower b values.

Keywords: breast cancer, b values, diffusion-weighted imaging, MRI

DOI:10.2214/AJR.09.2522

Received February 3, 2009; accepted after revision April 1, 2009.

[1]Clínica de Diagnóstico Por Imagem, Rua Ataulfo de Paiva, 669, 2nd floor, Leblon, Rio de Janeiro, RJ, Brazil, 22649-900. Address correspondence to F. P. A. Pereira (fephila@gmail.com).

[2]Multi-imagem Ressonância, Rio de Janeiro, RJ, Brazil.

[3]Department of Radiology, Federal University of Rio de Janeiro, Rio de Janeiro, RJ, Brazil.

[4]GE Healthcare, São Paulo, SP, Brazil.

AJR 2009; 193:1030–1035

0361–803X/09/1934–1030

MRI has high sensitivity (89–100%) but lacks specificity for characterizing breast tumors [1–5]. An overlap between the MRI findings of benign and malignant lesions still exists, resulting in variable specificity (50–90%) [3, 6–8]. This is caused by the false-positives related to the menstrual cycle, hormonal therapy, proliferative alterations, fibroadenomas, and papillomas. Because of this confounding overlap, in some cases it is not possible to make the differential diagnosis between benign and malignant lesions on the basis of conventional MRI features [9, 10]. Hence, several studies have investigated the role of advanced MRI techniques, such as diffusion-weighted imaging (DWI), to improve the specificity of MRI for the evaluation of breast lesions [9, 11–15].

DWI derives its image contrast from differences in the motion of water molecules (Brownian motion) in tissues. DWI is sensitive to the self-diffusion of water protons. As a result, it provides quantitative and qualitative information that reflects changes at a cellular level and unique insights about tumor cellularity and integrity of cell membranes. By using the DWI sequence, one can calculate the apparent diffusion coefficient (ADC), a quantitative measure that is directly proportional to the water diffusion [16]. High cell proliferation in malignant tumors increases cellular density, creating more barriers to the extracellular water diffusion, reducing the ADC, and resulting in signal loss. This sequence appears to be a useful tool for tumor detection and characterization [12], as well as for monitoring and predicting treatment response [17].

Recent studies have proven the potential of ADC to differentiate breast tumors [6, 11, 12]. These studies used different b values, varying from 0 to 1,000 s/mm^2, and found a significant difference of the ADC value between

malignant and benign lesions, with a sensitivity ranging from 81% to 93% and specificity from 80% to 88%, for an ADC cutoff of 1.1–1.3 × 10^{-3} mm^2/s. On clinical MRI scanners, diffusion sensitivity is easily altered by changing the parameter known as the b value, which is mainly proportional to the gradient amplitude and duration [17]. The images acquired with low b values are less diffusion-weighted because they use less gradient. On the other hand, the high b value images are strongly diffusion-weighted but have lower signal-to-noise ratio (SNR). The diffusion sensitivity is also affected by perfusion when low b values are used, producing higher ADC values.

DWI is typically performed using at least two b values to enable a meaningful interpretation. In theory, the error in ADC calculation can be reduced by using more b values. However, the more b values used, the longer the DWI sequence will be. Moreover, no consensus exists as to how many and which b values should be used in differentiating benign and malignant breast lesions using DWI.

This study aims to confirm the role of DWI for the differential diagnosis between benign and malignant breast lesions and to assess the best b values to be used for this differentiation.

Subjects and Methods

Study Population

From August 2007 to June 2008, this study prospectively enrolled 50 women with 57 focal breast lesions. Exclusion criteria were nonmass-like enhancement due to diffuse tumor spread and partial volume effect [13, 18]; benign cysts, because they do not present a diagnostic difficulty and their high ADC would artificially increase the mean and range of benign values [12]; patient movement that could lead to wrong ADC values; lesions not visible on the DWI sequence, mainly related to their small size (0.6 cm and 0.9 cm in our study); and neoadjuvant treatment before MRI, which could cause an increase in the ADC values [16, 19]. On the basis of these criteria, we excluded five lesions in five patients. As a result, the study included 45 patients (age range, 22–80 years; mean age, 46.1 years) with 52 breast lesions.

There were 26 malignant lesions on the histopathologic examination, including invasive ductal carcinoma (IDC) (n = 19), ductal carcinoma in situ (DCIS) (n = 2), tubular carcinoma (n = 2), adenoid cystic carcinoma (n = 1), mucinous colloid carcinoma (n = 1), and malignant phyllodes tumor (n = 1). The mean size of malignant lesions was 3.09 cm (range, 1.0–11.2 cm).

In addition, there were 26 benign lesions, of which six showed histopathologic results: fibroadenoma (n = 3), epidermoid cyst (n = 1), granulomatous intramammary lymph node (n = 1), and papilloma (n = 1). We also included 20 lesions classified as BI-RADS [20] category 2 by MRI to increase the benign lesion sample and to identify more reliable and representative ADC values. The diagnoses were defined by consensus of two experienced breast radiologists who had 11 and 8 years of experience. According to literature [21–23], the following criteria were considered predictive of benign disease: lobulated shape, smooth border, internal septations that do not enhance, the absence of enhancement, or enhancement less than that of the surrounding breast tissue. The presence of nonenhancing internal septations in a smooth or lobulated mass is highly specific for the diagnosis of fibroadenoma (93–97% specificity) [24, 25]. The mean size of benign lesions was 1.68 cm (range, 0.8–4.7 cm). In addition, after the 1-year follow-up with mammography or sonography, no significant modifications were seen in the imaging patterns of these benign lesions.

The study was approved by our institutional review board and all patients gave their informed consent.

MRI Acquisition

All MRI examinations were performed on a 1.5-T MR System (Signa Excite HD, GE Healthcare) with a bilateral 8-channel breast coil. Before DWI, standard sequences were acquired, including an axial T1-weighted spin-echo sequence (TR/TE, 370/15; echo-train length, 2; bandwidth, 41.67 MHz; matrix size, 512 × 256; field of view, 340 mm; number of signals averaged, 1; slice thickness, 5 mm; intersection gap, 1 mm), sagittal fat-suppressed T2-weighted fast spin-echo sequence (4,200/85; echo-train length, 19; bandwidth, 22.7 MHz; matrix size, 320 × 224; field of view, 220 mm; number of signals averaged, 2; slice thickness, 5 mm; intersection gap, 0 mm), axial STIR sequence (4,100/85; inversion time, 150 milliseconds; echo-train length, 17; bandwidth, 41.67 MHz; matrix size, 512 × 256; field of view, 340 mm; number of signals averaged, 2; slice thickness, 5 mm; intersection gap, 1 mm), and axial T1-weighted 3D fat-suppressed fast spoiled gradient-echo sequence (flip angle, 15°; bandwidth, 62.5 MHz; matrix size, 352 × 352; field of view, 350 mm; slice thickness, 1 mm; intersection gap, 0 mm) before and four times after the rapid injection of a bolus of 0.1 mmol/L of gadoterate meglumine (Dotarem, Guerbet) per kilogram of body weight followed by 20 mL of saline solution. After the examination, the unenhanced images were subtracted from the first and last contrast-enhanced images.

DWI was performed using an axial single-shot echo-planar imaging sequence centered on the lesions (b = 0, 250, 500, 750, and 1,000 s/mm^2; 1,800/93.8; echo-train length, 1; bandwidth, 25 MHz; matrix size, 160 × 192; field of view, 360 mm; number of signals averaged, 16; number of slices, 10; slice thickness, 5 mm; intersection gap, 0 mm; acquisition time, 3:44 minutes each for the five b values and 56 seconds when two b values were used).

MRI Analysis and Data Collection

All images were transferred to a workstation (Advantage Windows version 4.2_07, GE Healthcare) and the DWI sequence was postprocessed with commercial software (FuncTool, GE Healthcare) to obtain ADC maps (black-and-white and color, the latter with a Puh-thallium color scheme, ranging from black, diffusion restriction, to red, no diffusion restriction). The ADC maps of each lesion were calculated using five b values (0, 250, 500, 750, and 1,000 s/mm^2) and also using two b values, the b 0 s/mm^2 with each other b value separately (0 and 250 s/mm^2, 0 and 500 s/mm^2, 0 and 750 s/mm^2, 0 and 1,000 s/mm^2).

To achieve standardized conditions for analyses and to avoid contamination of the data by adjacent structures, two circular regions of interest (ROIs) having a mean diameter of 61 mm^2 (range, 40–94 mm^2) were individually placed in the target lesion in the same location as the five ADC maps cited above, and the average ADC was acquired for each b value combination. Apparent necrotic or cystic components were avoided by referring to conventional MR images.

Statistical Analysis

The data collected for this study included patient age, lesion size, BI-RADS classification, histopathologic result, ADC calculated with different b value combinations, and ROI sizes.

The Kolmogorov-Smirnov normality test was used to verify the fit of the variables age, tumor size, and ADC values to a normal distribution. All variables did not reject the hypothesis of normality, with a 5% significance level. The Student's t test was used to compare the means of age, tumor size, and ADC values in accordance with the benign or malignant diagnosis of the lesions. Before the t test, the Levene test had confirmed the equality of variances from these independent variables with a 5% significance level. The linear correlation between the five b value combinations (0, 250, 500, 750, and 1,000 s/mm^2, 0 and 250 s/mm^2, 0 and 500 s/mm^2, 0 and 750 s/mm^2, 0 and 1,000 s/mm^2) was tested using Spearman's nonparametric coefficient.

Receiver operating characteristic (ROC) analysis was carried out to determine a suitable ADC

value cutoff for each b value combination, so that benign and malignant lesions could be differentiated. The nonparametric distribution was the hypothesis used for the ROC curve. The comparison between the ROC curves was obtained through chi-square in the roccomp function. The best cutoff value was determined by Youden statistics—Y = sensitivity − (1 − specificity)—which allows a balance between good results of sensitivity and specificity. The highest value in Youden statistics indicates the best cutoff point and, consequently, the best sensitivity and specificity. CIs for sensitivity and specificity, using Wilson's formula, at level 95% were shown.

The statistical software (SPSS, version 16.0) was used for statistical analyses. Comparison of the ROC curves was done with commercial software (Stata 10.0 software). CIs for proportions were provided by software package DiagnosisMed from free software R, version 2.8.0 (CRAN, 2008).

All the variables that reached a significant p value (< 0.05) in the Student's t test independent samples, in the Spearman's correlation, and in the chi-square function were considered statistically significant.

TABLE 1: Apparent Diffusion Coefficient (ADC) Values of Benign and Malignant Lesions for Each b Value Combination

b Value Combinations (s/mm^2)	ADC Values ($\times 10^{-3}$ mm^2/s)								p
	Benign Lesions (n = 26)				Malignant Lesions (n = 26)				
	Mean	SD	Median	IQR	Mean	SD	Median	IQR	
0, 250, 500, 750, and 1,000	1.50	0.34	1.48	1.31–1.68	0.92	0.26	0.85	0.77–1.03	< 0.0001
0 and 250	1.77	0.44	1.67	1.55–1.97	1.25	0.28	1.18	1.03–1.39	< 0.0001
0 and 500	1.65	0.36	1.60	1.43–1.86	1.06	0.27	0.99	0.87–1.20	< 0.0001
0 and 750	1.58	0.31	1.54	1.37–1.78	0.96	0.24	0.88	0.83–1.04	< 0.0001
0 and 1,000	1.44	0.31	1.41	1.23–1.59	0.68	0.25	0.79	0.70–0.97	< 0.0001

Note—IQR = interquartile range.

TABLE 2: Apparent Diffusion Coefficient (ADC) in the Differentiation of Benign and Malignant Lesions for Each b Value Combination

b Value Combinations (s/mm^2)	Cutoff ($\times 10^{-3}$ mm^2/s)[a]	Sensitivity (%)	95% CI (%)	Specificity (%)	95% CI (%)	AUC[b]
0, 250, 500, 750 and 1,000	1.21	92.3 (2/26)	75.9–97.9	92.3 (2/26)	75.9–97.9	0.912
0 and 250	1.52	84.6 (4/26)	66.5–93.9	80.8 (5/26)	62.1–91.5	0.866
0 and 500	1.36	92.3 (2/26)	75.9–97.9	84.6 (4/26)	66.5–93.9	0.919
0 and 750	1.24	92.3 (2/26)	75.9–97.9	96.2 (1/26)	81.1–99.3	0.942
0 and 1,000	1.14	92.3 (2/26)	75.9–97.9	88.5 (3/26)	71.0–96.0	0.937

Note—Numbers in parentheses are numbers of patients.
[a]ADC cutoff value.
[b]Area under ROC curve; represents probability that ADC value will accurately characterize a breast lesion as malignant or benign according to cutoff value.

Results

The mean ADC obtained from malignant breast lesions (mean, 0.68–1.25 ± 0.25–0.28 [SD] × 10^{-3} mm^2/s) was significantly lower than that observed in benign lesions (mean, 1.44–1.77 ± 0.31–0.44 × 10^{-3} mm^2/s) in all b value combinations (p < 0.0001), whether five b values or a b value of 0 s/mm^2 was used with each other b value separately to calculate the ADC (Table 1).

All the b value combinations used to calculate the ADC showed high sensitivity and specificity for the differentiation of benign and malignant lesions, with no significant difference (p = 0.2581) (Table 2, Figs. 1 and 2). The ADC calculated from b values of 0 and 750 s/mm^2 was slightly better than the other b value combinations. Considering a cutoff value of 1.24 × 10^{-3} mm^2/s for ADC calculated from b values of 0 and 750 s/mm^2, one of 26 benign lesions (papilloma) and two of 26 malignant lesions (mucinous colloid carcinoma and malignant phyllodes tumors) would be misdiagnosed, with a sensitivity of 92.3% and a specificity of 96.2%. The ADC calculated from b values of 0 and 250 s/mm^2 was the worst in the differentiation of benign and malignant lesions, showing a sensitivity of 84.6% and a specificity of 80.8%, with a cutoff value of 1.52 × 10^{-3} mm^2/s.

The Spearman's correlations between the ADCs obtained with the five different b value combinations were positive and statistically significant (p < 0.0001), showing coefficients greater than 0.90. The highest coefficients obtained were 0.98 by the correlation between the five b values and b 0 and 1,000 s/mm^2, 0.96 by the correlation between b 0 and 750 s/mm^2 and b 0 and 1,000 s/mm^2, and 0.95 by the correlation between the five b values and b 0 and 750 s/mm^2. The lowest coefficient was 0.89, calculated by the correlation between b 0 and 250 s/mm^2 and b 0 and 750 s/mm^2.

Discussion

In this study, we evaluated the role of DWI in distinguishing benign from malignant breast lesions and assessed the best b values to be used for the differentiation. The mean ADC value of the benign lesions was significantly lower than that of the malignant lesions for all b value combinations studied. Moreover, no statistical difference was seen in the ADC values calculated from the different b value combinations studied.

DWI reflects changes in water molecule mobility caused by alterations of the tissue environment due to a pathologic process. Therefore, measurement of the motion of water molecules can provide an additional feature that may further increase the specificity of the MRI classification of breast lesions. Prior studies with breast MRI and DWI have shown promising results in differentiating benign and malignant lesions, with sensitivity ranging from 81% to 93% and specificity from 80% to 88.5% [6, 11–14, 26, 27]. Our results corroborate those of previous studies. We obtained ADC values calculated from different b value combinations, and all of them revealed a statistically significant difference between benign and malignant lesions.

However, there are still no studies in literature suggesting the best b values to be used when calculating the ADC of normal and abnormal breast tissue. The b value chosen can interfere with diffusion sensitivity because the water molecules with a large degree of motion (e.g., in the intravascular space) will show signal attenuation with small b values. For this reason, the ADC is strongly affected by vascular perfusion in the case of small b values, and it tends to be higher when measured

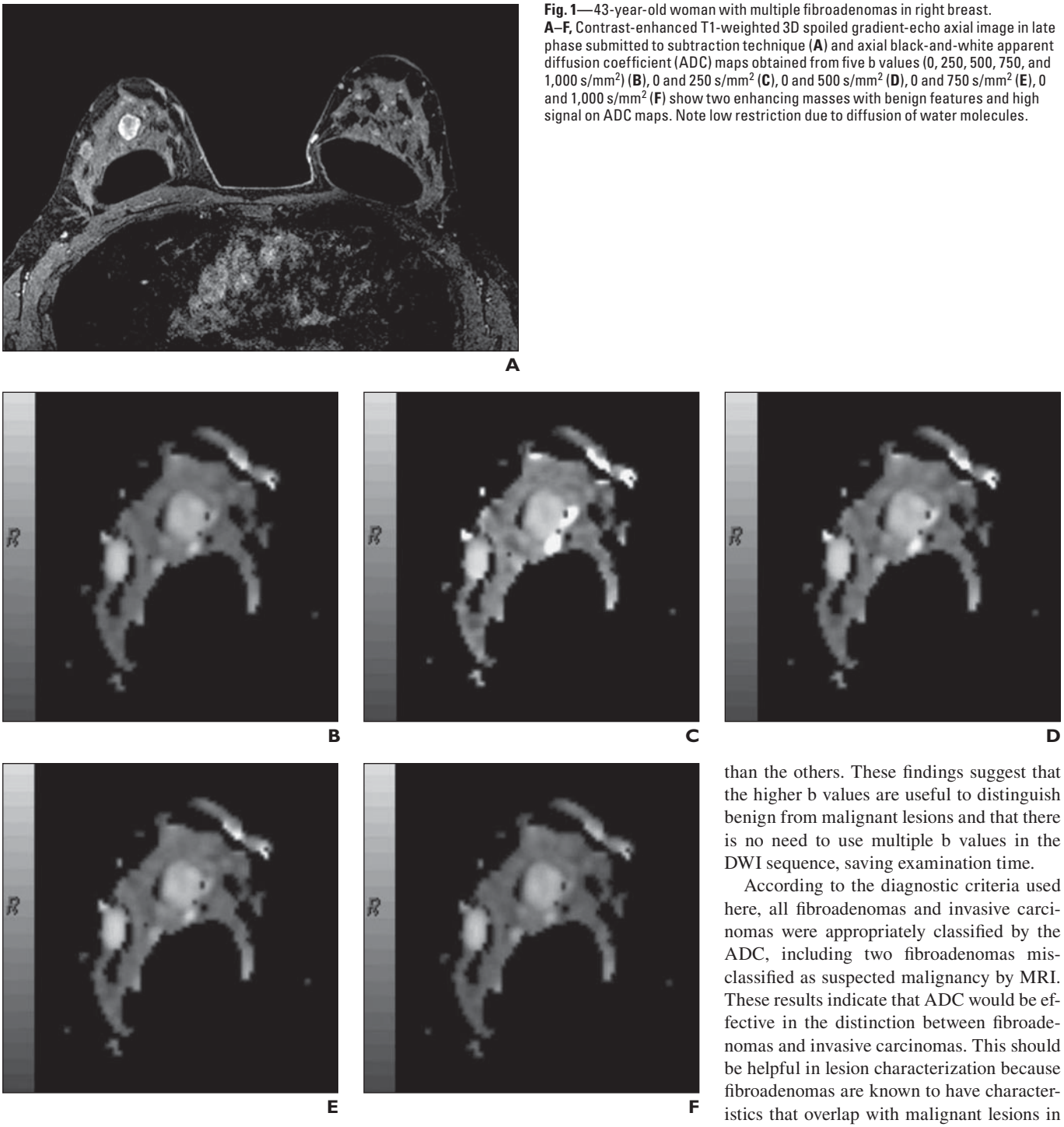

Fig. 1—43-year-old woman with multiple fibroadenomas in right breast. **A–F,** Contrast-enhanced T1-weighted 3D spoiled gradient-echo axial image in late phase submitted to subtraction technique (**A**) and axial black-and-white apparent diffusion coefficient (ADC) maps obtained from five b values (0, 250, 500, 750, and 1,000 s/mm^2) (**B**), 0 and 250 s/mm^2 (**C**), 0 and 500 s/mm^2 (**D**), 0 and 750 s/mm^2 (**E**), 0 and 1,000 s/mm^2 (**F**) show two enhancing masses with benign features and high signal on ADC maps. Note low restriction due to diffusion of water molecules.

only with small b values [10, 11, 13, 15, 28]. By contrast, it is clear that in high b values, the SNR is decreased [10, 15], which can also interfere with the ADC. In addition, although in theory an ADC calculation error might be reduced by using more b values [17], no previous studies have tested this hypothesis when assessing DWI of the breast. In our study, in comparing the ADC calculated from different b values, lower b values showed a higher ADC and vice versa. Nevertheless, there was no statistical difference between the ADC of different b value combinations in the differentiation between benign and malignant lesions. The ADC calculated from b 0 and 750 s/mm^2 was slightly better than the others. These findings suggest that the higher b values are useful to distinguish benign from malignant lesions and that there is no need to use multiple b values in the DWI sequence, saving examination time.

According to the diagnostic criteria used here, all fibroadenomas and invasive carcinomas were appropriately classified by the ADC, including two fibroadenomas misclassified as suspected malignancy by MRI. These results indicate that ADC would be effective in the distinction between fibroadenomas and invasive carcinomas. This should be helpful in lesion characterization because fibroadenomas are known to have characteristics that overlap with malignant lesions in both ultrasound and dynamic contrast-enhanced MRI studies [15, 29, 30].

Our results confirmed that the mean ADC of breast tumors correlates well with tumor cellularity, even when evaluating the false-positives and false-negatives. Malignant breast tumors have a higher cellularity and a lower ADC than benign breast tumors. Hence, a malignant tumor with low cellularity, such as the malignant

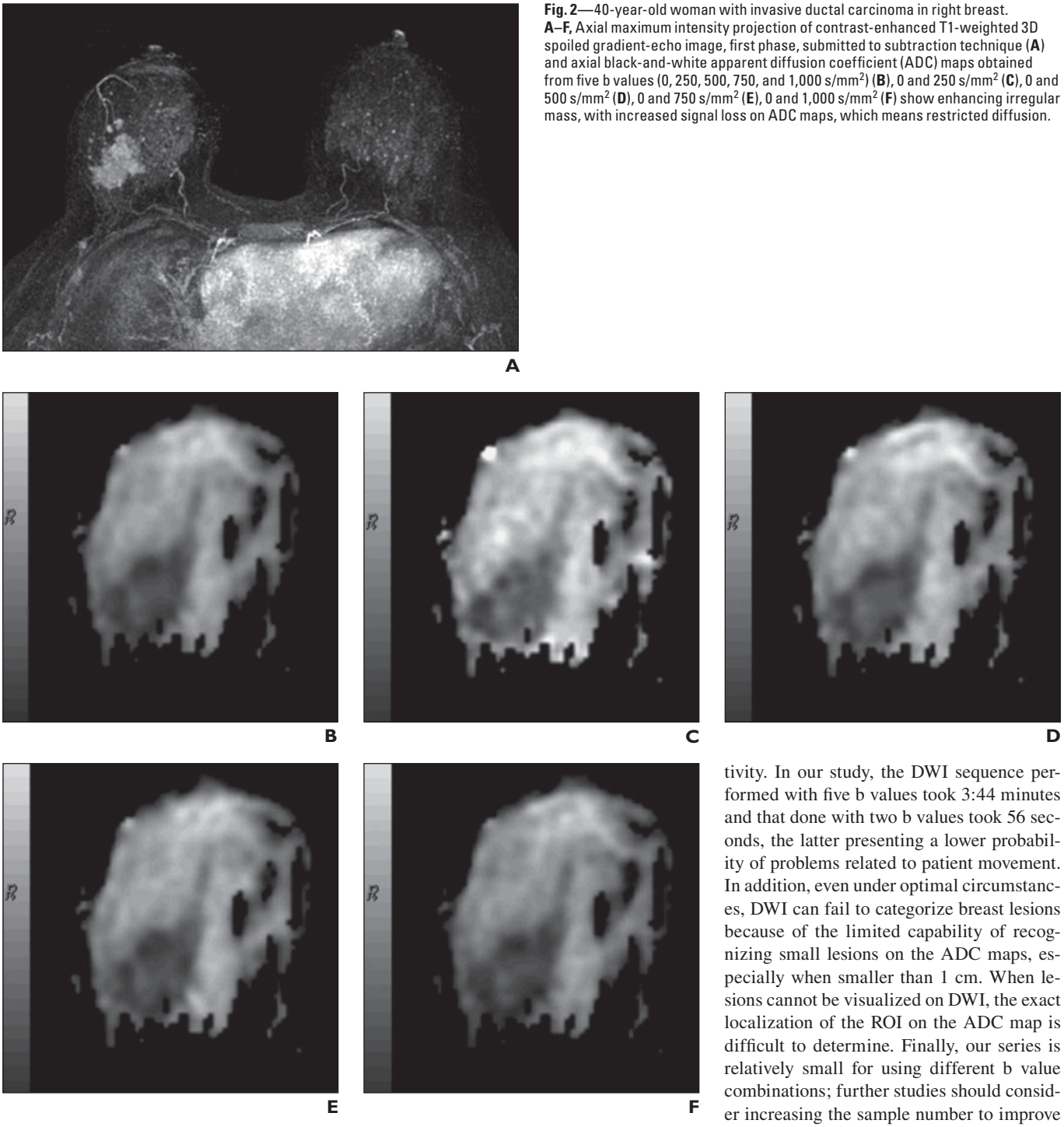

Fig. 2—40-year-old woman with invasive ductal carcinoma in right breast. **A–F,** Axial maximum intensity projection of contrast-enhanced T1-weighted 3D spoiled gradient-echo image, first phase, submitted to subtraction technique (**A**) and axial black-and-white apparent diffusion coefficient (ADC) maps obtained from five b values (0, 250, 500, 750, and 1,000 s/mm^2) (**B**), 0 and 250 s/mm^2 (**C**), 0 and 500 s/mm^2 (**D**), 0 and 750 s/mm^2 (**E**), 0 and 1,000 s/mm^2 (**F**) show enhancing irregular mass, with increased signal loss on ADC maps, which means restricted diffusion.

phyllodes tumor with cystic areas seen in our series, which shows high ADC, consequently was misdiagnosed as benign. A carcinoma with a very high signal intensity on T2-weighted images—such as mucinous colloid carcinoma—resulted in misleading ADC values because of a lower cell density and higher extracellular water content [31, 32]. Conversely, a benign tumor with high cellularity, such as the papilloma seen in our study, showed low ADC and led to the misdiagnosis of malignancy.

Our study had some limitations. First, patient movement during the acquisition of the DWI sequences leads to wrong ADC values. The longer acquisition time caused by the use of more b values may lead to patient activity. In our study, the DWI sequence performed with five b values took 3:44 minutes and that done with two b values took 56 seconds, the latter presenting a lower probability of problems related to patient movement. In addition, even under optimal circumstances, DWI can fail to categorize breast lesions because of the limited capability of recognizing small lesions on the ADC maps, especially when smaller than 1 cm. When lesions cannot be visualized on DWI, the exact localization of the ROI on the ADC map is difficult to determine. Finally, our series is relatively small for using different b value combinations; further studies should consider increasing the sample number to improve the statistical power.

Despite these limitations, DWI of the breast provides additional information to characterize focal breast lesions in a fast and easy way. In this series, we obtained sensitivity and specificity as high as 92% and 96%, respectively, with a cutoff ADC value of 1.24×10^{-3} mm^2/s (b 0 and 750 s/mm^2) for the diagnosis of benign and malignant lesions.

Thus, by combining ADC measurements and dynamic studies with interpretation of enhancement patterns, the latter known to have good sensitivity but variable specificity for characterizing lesions, the overall accuracy of MRI can be increased, reducing unnecessary invasive procedures. Nevertheless, further studies with larger populations are needed to confirm the use of DWI in the evaluation of breast lesions.

In addition, our study showed similar results when using two or five b values to calculate the ADC for the differentiation between benign and malignant lesions. This is important because the sequence with fewer b values can save examination time and reduce the probability of movement artifacts.

References

1. Kuhl C. The current status of breast MR imaging. Part I. Choice of technique, image interpretation, diagnostic accuracy, and transfer to clinical practice. *Radiology* 2007; 244:356–378
2. Schnall MD, Blume J, Bluemke DA, et al. Diagnostic architectural and dynamic features at breast MR imaging: multicenter study. *Radiology* 2006; 238:42–53
3. Macura KJ, Ouwerkerk R, Jacobs MA, Bluemke DA. Patterns of enhancement on breast MR images: interpretation and imaging pitfalls. *RadioGraphics* 2006; 26:1719–1734
4. Wierner JI, Schilling KJ, Adami C, Obuchowski NA. Assessment of suspected breast cancer by MRI: a prospective clinical trial using a combined kinetic and morphologic analysis. *AJR* 2005; 184: 878–886
5. Bedrosian I, Mick R, Orel SG, et al. Changes in the surgical management of patients with breast carcinoma based on preoperative magnetic resonance imaging. *Cancer* 2003; 98:468–473
6. Marini C, Iacconi C, Giannelli M, Cilotti A, Moretti M, Bartolozzi C. Quantitative diffusion-weighted MR imaging in the differential diagnosis of breast lesion. *Eur Radiol* 2007; 17:2646–2655
7. Kuhl CK, Mielcareck P, Klaschik S, et al. Dynamic breast MR imaging: are signal intensity time course data useful for differential diagnosis of enhancing lesions? *Radiology* 1999; 211:101–110
8. Fischer U, Kopka L, Grabbe E. Breast carcinoma: effect of preoperative contrast-enhanced MR imaging on the therapeutic approach. *Radiology* 1999; 213:881–888
9. Wenkel E, Geppert C, Schulz-Wendtland R, et al. Diffusion weighted imaging in breast MRI: comparison of two different pulse sequences. *Acad Radiol* 2007; 14:1077–1083
10. Sinha S, Sinha U. Functional magnetic resonance of human breast tumors: diffusion and perfusion imaging. *Ann N Y Acad Sci* 2002; 980:95–115
11. Guo Y, Cai YQ, Cai ZL, et al. Differentiation of clinically benign and malignant breast lesions using diffusion-weighted imaging. *J Magn Reson Imaging* 2002; 16:172–178
12. Rubesova E, Grell AS, De Maertelaer V, Metens T, Chao SL, Lemort M. Quantitative diffusion imaging in breast cancer: a clinical prospective study. *J Magn Reson Imaging* 2006; 24:319–324
13. Woodhams R, Matsunaga K, Iwabuchi K, et al. Diffusion-weighted imaging of malignant breast tumors: the usefulness of apparent diffusion coefficient (ADC) value and ADC map for the detection of malignant breast tumors and evaluation of cancer extension. *J Comput Assist Tomogr* 2005; 29:644–649
14. Kuroki Y, Nasu K, Kuroki S, et al. Diffusion-weighted imaging of breast cancer with the sensitivity encoding technique: analysis of the apparent diffusion coefficient value. *Magn Reson Med Sci* 2004; 3:79–85
15. Sinha S, Lucas-Quesada FA, Sinha U, et al. In vivo diffusion-weighted MRI of the breast: potential for lesion characterization. *J Magn Reson Imaging* 2002; 15:693–704
16. Paran Y, Bendel P, Margalit R, Degani H. Water diffusion in the different microenvironments of breast cancer. *NMR Biomed* 2004; 17:170–180
17. Koh DM, Collins DJ. Diffusion-weighted MRI in the body: applications and challenges in oncology. *AJR* 2007; 188:1622–1635
18. Kuroki-Suzuki S, Kuroki Y, Nasu K, Nawano S, Moriyama N, Okazaki M. Detecting breast cancer with non-contrast MR-imaging: combining diffusion-weighted and STIR imaging. *Magn Reson Med Sci* 2007; 6:21–27
19. Pickles MD, Gibbs P, Lowry M, Turnbull LW. Diffusion changes precede size reduction in neoadjuvant treatment of breast cancer. *Magn Reson Imaging* 2006; 24:843–847
20. American College of Radiology (ACR). ACR BI-RADS: magnetic resonance imaging. In: *ACR breast imaging reporting and data system, breast imaging atlas.* Reston, VA: American College of Radiology, 2003
21. Kuhl, CK. Concepts for differential diagnosis in breast MR imaging. *Magn Reson Imaging Clin N Am* 2006; 14:305–328
22. Morris, EA. Breast MR imaging lexicon updated. *Magn Reson Imaging Clin N Am* 2006; 14:293–303
23. Schnall M, Orel S. Breast MR imaging in the diagnostic setting. *Magn Reson Imaging Clin N Am* 2006; 14:329–337
24. Nunes LW, Schnall MD, Siegelman ES, et al. Diagnostic performance characteristics of architectural features revealed by high-spatial-resolution MR imaging of the breast. *AJR* 1997; 169:409–415
25. Nunes LW, Schnall MD, Orel SG, et al. Correlation of lesion appearance and histologic findings for the nodes of a breast MR imaging interpretation model. *RadioGraphics* 1999; 19:79–92
26. Yabuuchi H, Matsuo Y, Okafuji T, et al. Enhanced mass on contrast-enhanced breast MR imaging: lesion characterization using combination of dynamic contrast-enhanced and diffusion-weighted MR images. *J Magn Reson Imaging* 2008; 28:1157–1165
27. Park MJ, Cha ES, Kang BJ, Ihn YK, Baik JH. The role of diffusion-weighted imaging and the apparent diffusion coefficient (ADC) values for breast tumors. *Korean J Radiol* 2007; 8:390–396
28. Yoshikawa MI, Ohsumi O, Sugata S, et al. Comparison of breast cancer detection by diffusion-weighted magnetic resonance imaging and mammography. *Radiat Med* 2007; 25:218–223
29. Stomper PC, Winston JS, Hermann S, Klippenstein DL, Arredondo MA, Blumenson LE. Angiogenesis and dynamic MR imaging gadolinium enhancement of malignant and benign breast lesions. *Breast Cancer Res Treat* 1997; 45:39–46
30. Hochman MG, Orel SG, Powell CM, Schnall MD, Reynolds CA, White LN. Fibroadenomas: MR imaging appearances with radiologic–histopathologic correlation. *Radiology* 1997; 204:123–129
31. Kawashima M, Tamaki Y, Nonaka T, et al. MR imaging of mucinous carcinoma of the breast. *AJR* 2002; 179:179–183
32. Hatakenaka M, Soeda H, Yabuuchi H, et al. Apparent diffusion coefficients of breast tumors: clinical application. *Magn Reson Med Sci* 2008; 7:23–29